A Fast Deterministic Algorithm for Side Lobe Level Reduction of Open Loop Coplanar Distributed Antenna Arrays in WSNs

Haythem H. Abdullah[1], Heba S. Dawood[2], and Amr H. Hussein[2, *]

Abstract—Distributed beamforming (DBF) is an efficient technique for reliable communications in wireless sensor networks (WSNs). In DBF based networks, the randomly distributed nodes cooperate to form a randomly distributed antenna array (RAA) which has a main beam directed towards the intended receiver. Due to the nodes randomness, the DBF results in poor pattern characteristics such as high side lobe level (SLL) and pattern asymmetry around the main beam sides. In this paper, a fast deterministic algorithm for SLL reduction of open loop distributed antenna arrays is introduced. Unlike the existing state of the art optimization techniques for SLL reduction, the proposed algorithm provides a fast deterministic solution for energy transmission or the weight of each node without changing its location. Consequently, the exhaustive search burden of the optimization based techniques for the optimum weights is avoided. The simulation results reveal that the proposed algorithm has superior performance to the optimization techniques in terms of execution time, synthesized SLL, and half power beamwidth (HPBW).

1. INTRODUCTION

The traditional antenna arrays consisting of periodic structures such as linear, planar, and circular antenna arrays configurations suffer from scan blindness problem and tight fabrication constraints [1]. Also, the utilization of co-located antennas or traditional arrays in wireless communication systems may lead to significant frequency selective fading, limited transmit power, limited bandwidth, and reduced system capacity. As a promising solution for these critical problems, the distributed antenna networks have been introduced in [2]. In the same context, the distributed Multi-input Multi-output (D-MIMO) has been introduced in [3] for further enhancement of the spectral and energy efficiency of the conventional co-located MIMO (C-MIMO). Wireless Sensor Networks (WSNs) consist of a large number of sensor nodes distributed over a specific area. The nodes are collaborating together for sensing, collecting, and processing information. They have a limited power supply and can't transmit a signal for a long distance [4]. Distributed beamforming is the key solution for mitigating these problems. In DBF, each sensor node acts as a virtual antenna element to construct a randomly distributed antenna array (RAA). However, the randomness of the distributed nodes creates an array pattern having a high SLL which causes high interference with the unintended receivers located within the same region as well as reducing the received power level at the intended receiver [5, 6]. The interference with the unintended receivers limits the system capacity and increases the bit error rate. As antenna arrays with low side lobe levels are required for efficient and reliable communications, many research works are introduced for SLL reduction of distributed antenna arrays. In [7], a node selection based technique for SLL reduction was introduced. It is mainly based on selecting a combination of nodes from the available set of nodes in the WSN and determines the nodes weights according to their locations.

* Corresponding author: Amr Hussein Hussein Abdullah (amrvips@yahoo.com, amr.abdallah@f-eng.tanta.edu.eg).
[1] Electronics Research Institute, El-Tahreer St. Dokki, Giza, Egypt. [2] Electronics and Electrical Communications Engineering Department, Faculty of Engineering Tanta University, Tanta, Egypt.

However, it depends on the MAC protocol and one-bit feedback from the unintended receiver which is impossible in some cases. In [8], a modified version of the node selection technique denoted as Bat-Chicken Swarm Optimization (BATCSO) was introduced. It tends to optimize the peak SLL of the array pattern by controlling the nodes transmission energies. A long these lines, a Genetic Algorithm (GA) based technique for SLL minimization was introduced in [9]. It synthesizes the transmission energy of each node without changing the nodes locations. It provides better performance compared to the conventionally distributed beamforming (CDBF). In [10], two Weightless Swarm Algorithm (WSA) and Particle Swarm Optimization (PSO) based techniques were introduced for SLL reduction by adjusting the nodes transmission energy. But, they suffer from increased computational complexity. The WSA based technique provided higher SLL reduction than GA and PSO based techniques which consequently improves the signal to noise and interference ratio (SINR) and the capacity of unintended receivers. Along these lines, PSO and Gravitational Search Algorithm (GSA) based SLL reduction techniques were introduced in [11]. They control both transmission energy and transmission phase of each node without any changes in the nodes locations. In [12], a hybrid meta-heuristic optimization algorithm denoted as (PSOGSA-E) which is a combination between the PSO and GSA-Explore was introduced. It suppresses the SLL by optimizing the weight (amplitude and phase) of each node in the RAA. Also, the Non-dominated Sorting GA with selective distance (NSGA-SD) algorithm was introduced in [13]. It provides a bi-objective optimization formulation for the DBF. It controls the weight (amplitude and phase) of each node to minimize the SLL and at the same time maximizes the directivity of the array pattern. But, it is worth pointing to that all the aforementioned SLL reduction techniques which are based on optimization algorithms are time consuming.

There are several applications such as satellite communications, radar systems, and wireless sensor networks where large arrays sizes are very critical to achieve the desired radiation patterns to fulfill the required systems performances. However, large antenna arrays based systems have large computation burden, complex RF front end chains, and high power consumption. To mitigate these problems, adaptive beamforming making the use of sparse characteristics of large antenna arrays based systems is the key solution. In [14], an efficient l_0-norm constrained normalized least-mean-square (L_0-CNLMS) adaptive beamforming algorithm for controllable sparse antenna arrays was introduced. It is suitable for sparse antenna arrays of different configurations such as standard hexagonal array (SHA) used in satellite communications, rectangular array (RA) used for C-band based radar systems, triangular array (TA) used for P-band based stealth aircraft and satellite detection systems, and irregular arrays (IA) used for S-band communications. Also, it converges faster and utilizes fewer number of antenna elements compared to state of the art sparsity based adaptive beamforming algorithms. However, for non-sparse arrays, its performance is degraded and provides high SLL compared to the conventional non-sparse beamforming algorithms. In the same context, several sparsity based optimization filtering algorithms can be utilized in the SLL reduction as introduced in [15–17]. These algorithms have proved their effectiveness in the well-defined antenna arrays structures such as linear and planar configurations. However, they have to be modified to be applied to randomly distributed antenna arrays. In RAAs, the randomness of nodes distribution may make the separation distances between some of the array nodes to be small enough to maximize the mutual coupling between the neighboring nodes. Several techniques have been introduced to minimize the coupling effect between the antenna arrays elements as in [18] and [19].

In this paper, a fast deterministic DBF algorithm for maximum SLL reduction of open loop distributed antenna arrays is introduced. It determines the transmission energy of each node without inspiring the node location. It saves the computation time and search burden of the best weights required to synthesize the desired pattern, especially for large size RAAs. Also, it does not require feedback from the unintended receivers. The simulation results revealed that the proposed technique outperforms the recent state of the art optimization based SLL reduction techniques which handle the nodes weights. It is suitable for the distributed automotive 77 GHz radar sensors. The existing low power 77 GHz radar sensors suffer from their limited detection range. To extend the radar range, some randomly distributed sensors within a specific area can be grouped to form a RAA to take the advantage of array gain in increasing the radar range. This work is done under the contract between the National Telecom Regulatory Authority (NTRA), Ministry of Communications and Information Technology (MCIT), Egypt and the Electronics Research Institute (ERI), Ministry of scientific research, Egypt start date

2018. The paper is organized as follows. In Section 2, the system model is introduced. The proposed SLL reduction algorithm is presented in Section 3. The simulation results are illustrated in Section 4. Finally, the paper is concluded in Section 5.

2. SYSTEM MODEL

In this section, the geometrical configuration of distributed antenna arrays is introduced. Consider K nodes which are distributed over a circular disk of radius R meters. Each node has polar coordinates (r_k, ψ_k) where r_k is the distance of the kth node from the central point of the cluster, $r_k \in [0, R]$, and ψ_k is the azimuth angle of the kth node with respect to x-axis, $\psi_k \in [-\pi, \pi]$. It is assumed that all nodes are isotropic antennas and coplanar with each other. Furthermore, all nodes are perfectly synchronized in phase, time, and frequency. Assume that an intended receiver exists in the proximity of other unintended receivers distributed randomly in space as shown in Fig. 1. The intended receiver has spherical coordinates (A, θ_0, φ_0), where A is the distance between the intended receiver and the central point of the RAA, θ_0 the elevation direction, $\theta_0 \in [0, \pi]$, and φ_0 the azimuth direction, $\varphi_0 \in [-\pi, \pi]$ of the intended receiver. The spherical coordinates of the L unintended receivers are $(A_l, \theta_l, \varphi_l)$, $l = 1, 2, \dots L$, where A_l is the distance between the unintended receiver and the central point of the RAA, θ_l the elevation direction, $\theta_l \in [0, \pi]$, and φ_l the azimuth direction, $\varphi_l \in [-\pi, \pi]$ of the unintended receivers. Also, assume that the intended and unintended receivers are located within the same plane as the distributed nodes where $\theta_0 = \theta_l = \frac{\pi}{2}$. Fig. 1 shows the geometrical structure of distributed antenna array [5].
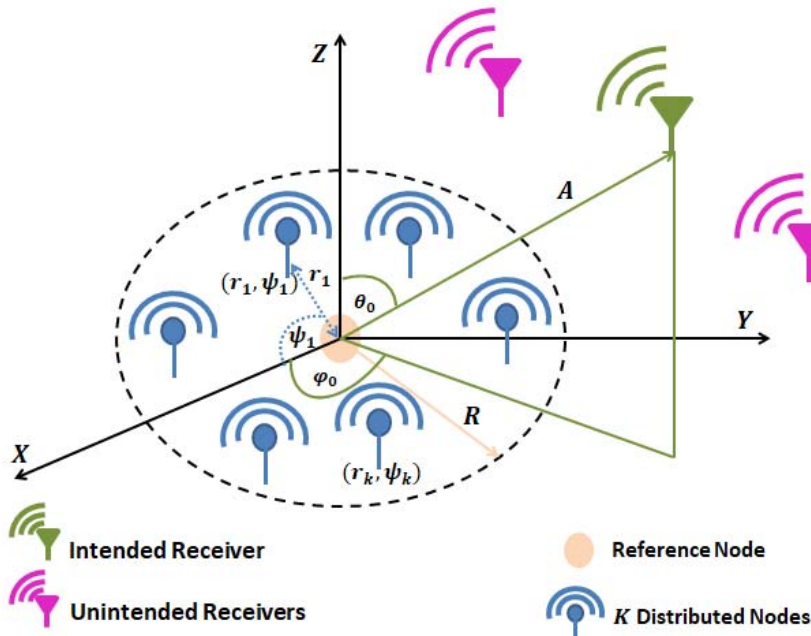

Figure 1. Geometrical structure of the distributed antenna array.

3. PROPOSED SLL REDUCTION ALGORITHM

In WSNs, to mitigate the high interference with the unintended receivers and increase the received power level at the intended receiver, SLL reduction is the key solution. It significantly improves the capacity and the bit error rate performance of the network. In this section, the proposed algorithm for SLL reduction of RAAs is introduced. The steps of the proposed algorithm are presented as follows:

Consider an ordinary RAA consisting of K nodes distributed over a circular disk of radius R with coordinates $r = [r_1, r_2, \dots, r_K]$ and $= [\psi_1, \psi_2, \dots, \psi_K]$ where r_k and ψ_k are the radius and angle of the

k^{th} node with respect to the center point of the RAA, respectively and $k = 1, 2, 3, \ldots K$. The array pattern of the RAA, $AF(\varphi)$ is given by [5]:

$$AF(\varphi) = \frac{1}{K} \sum_{k=1}^{K} w_k e^{-j\frac{2\pi}{\lambda}r_k \cos(\varphi - \psi_k)} \tag{1}$$

where w_k is the transmission weight of the kth node which is given by:

$$w_k = \xi_k e^{j\Psi_k} \tag{2}$$

where ξ_k and Ψ_k are the kth node transmission energy amplitude and initial transmission phase, respectively. For a uniformly fed array, $\xi_k = 1$ and Ψ_k is determined by [5] as follows:

$$\Psi_k = \frac{2\pi}{\lambda}r_k \cos(\varphi_0 - \psi_k) \tag{3}$$

It is required to synthesize an array pattern which has a main beam directed towards the intended receiver with minimum SLL. In this case, the desired array pattern, $AF_d(\varphi)$, can be defined as follows:

$$AF_d(\varphi) = \begin{cases} 0, & -\pi \leq \varphi < \varphi_{NL1} \\ AF(\varphi), & \varphi_{NL1} \leq \varphi \leq \varphi_{NL2} \\ 0, & \varphi_{NL2} < \varphi \leq \pi \end{cases} \tag{4}$$

where φ_{NL1} and φ_{NL2} are the angles of the first two nulls of the ordinary array pattern $AF(\varphi)$. For clarification, consider the ordinary array pattern for $K = 16$ elements, $R = 1\,\text{m}$, and the main beam is directed at $\varphi_0 = 0°$. Then, the desired array pattern $AF_d(\varphi)$ is plotted as shown in Fig. 2.
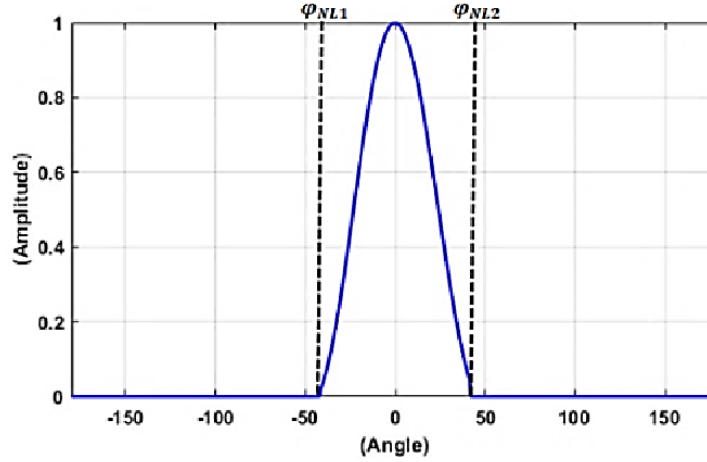

Figure 2. The desired array pattern $AF_d(\varphi)$ for $K = 16$ elements, $R = 1\,\text{m}$ and the main beam directed at $\varphi_0 = 0°$.

The synthesized array pattern $AF_{syn}(\varphi)$ should have the same characteristics as the desired array pattern $AF_d(\varphi)$ such that:

$$AF_{syn}(\varphi) = \frac{1}{K} \sum_{k=1}^{K} v_k e^{-j\frac{2\pi}{\lambda}r_k \cos(\varphi - \psi_k)} \cong AF_d(\varphi) \tag{5}$$

where v_k is the synthesized transmission weight of the kth node which equals $\delta_k e^{j\Psi_k}$. δ_k is the synthesized transmission energy of the kth node, while the initial transmission phase Ψ_k of the kth node remains fixed as defined in Eq. (3). Substituting v_k in Eq. (5), the synthesized array pattern is rewritten as

$$AF_{syn}(\varphi) = \frac{1}{K} \sum_{k=1}^{K} \delta_k e^{j\Psi_k} e^{-j\frac{2\pi}{\lambda}r_k \cos(\varphi - \psi_k)} \cong AF_d(\varphi) \tag{6}$$

To estimate the transmission energy of each node, δ_k, Eq. (6) is transformed into a matrix form as follows:

$$[\delta]_{1 \times K} \times [S]_{K \times N} = [U]_{1 \times N} \tag{7}$$

or for simplicity Eq. (7) is written as:

$$\delta S = U \tag{8}$$

where N is the number of samples of the desired pattern $AF_d(\varphi)$. The number of samples is chosen to be large enough to maintain the pattern smoothness and details. For a given number of samples, N, the sample angles of $\varphi \in [-\pi, \pi]$ can be calculated by:

$$\varphi_n = \frac{2n\pi}{N}, \quad n = 1, 2, 3, \ldots N \tag{9}$$

The elements of $[U]_{1 \times N}$ vector are the samples of the desired pattern $AF_d(\varphi)$ at the sample angle φ_n within the range $-\pi \leq \varphi \leq \pi$ and can be defined as:

$$[U]_{1 \times N} = [AF_d(\varphi_1) \, AF_d(\varphi_2) \ldots AF_d(\varphi_N)] \tag{10}$$

δ is the $(1 \times K)$ vector of the synthesized transmission energies of the distributed nodes which is given by

$$\delta = [\delta_1 \delta_2 \ldots \delta_K] \tag{11}$$

S is a $K \times N$ matrix whose elements are given by

$$S_{kn} = \frac{1}{K} e^{j\Psi_k} e^{-j\frac{2\pi}{\lambda} r_k \cos(\varphi_n - \psi_k)}, \quad k = 1, 2, \ldots, K \quad \text{and} \quad n = 1, 2, \ldots, N \tag{12}$$

The synthesized transmission energy vector can be obtained by solving Eq. (8). As S is a non-square matrix, both sides of Eq. (8) are multiplied by the Hermitian transpose of the matrix S which is denoted as S^H. Then Eq. (8) is written as:

$$\delta S S^H = U S^H \tag{13}$$

Let $R_{SS} = SS^H$ which is a $K \times K$ square matrix. Then Eq. (13) can be rewritten as:

$$\delta R_{SS} = U S^H \tag{14}$$

Multiplying both sides of Eq. (14) by the inverse of the R_{SS} matrix, the synthesized transmission energy vectorcan be calculated by:

$$\delta = U S^H R_{SS}^{-1} \tag{15}$$

where R_{SS}^{-1} is the inverse of the square matrix R_{SS}.

4. SIMULATION RESULTS

In this section, several simulations are carried out to evaluate and compare the performance of the proposed algorithm with that of the GA based synthesis techniques introduced in [9, 10] and that of the NSGA-SD algorithm introduced in [13]. The GA is utilized to synthesize the antenna array for the maximum SLL reduction by optimizing the transmission energy δ which minimizes the following cost function.

$$CF(\delta) = 20\log_{10} \frac{\max(AF(\varphi_{SL}))}{AF(\varphi_{ML})} \tag{16}$$

where $AF(\varphi_{SL})$ is the amplitude of the array pattern at the side lobe angle φ_{SL} which is defined as $\varphi_{SL} \in [(-\pi, \varphi_{NL1}) \cup (\varphi_{NL2}, \pi)]$, while $AF(\varphi_{ML})$ is the amplitude of the array pattern at the main lobe angle φ_{ML}. Also, the maximum number of iterations (I_{ga}) of the GA is limited to $I_{ga} = 100$ as introduced in [9, 10]. In the simulations, the number of array pattern samples is set to $N = 1000$ samples for the proposed algorithm and the other algorithms of comparison introduced in [9], [10], and [13]. The simulations are carried out using MATLAB R2016a on ASUS laptop intel core i5-5200U. The simulation results are divided into two sections; Section 1 handles the analysis of the synthesized array pattern, and Section 2 handles the analysis of the SLL under the impact of the variations in the number of nodes, K, and the circular area radius, R.

4.1. Synthesized Array Pattern Analysis

In this section, the synthesized array patterns using the proposed algorithm, GA, and NSGA-SD optimization based techniques are compared with the ordinary array pattern in terms of the maximum SLL, HPBW, execution time, and dynamic range ratio (DRR) which is defined as:

$$DRR = \frac{maximum\ transmission\ energy}{minimum\ transmission\ energy} = \frac{\delta_{\max}}{\delta_{min}} \tag{17}$$

Four test cases are considered using a small number of nodes distributed over a small circular area of radius R, i.e., ($K = 16$ and $R = 1\,\mathrm{m}$), ($K = 8$ and $R = 1\,\mathrm{m}$), and using a large number of nodes distributed over a moderate area, i.e., ($K = 32$ and $R = 4\,\mathrm{m}$) and ($K = 64$ and $R = 6\,\mathrm{m}$).

Test case (1): in this case, consider a $K = 16$ distributed antenna array whose nodes are randomly distributed over a small circular disk area of radius $R = 1\,\mathrm{m}$ as shown in Fig. 3. The direction of the intended receiver is at the azimuth angle $\varphi_0 = 0°$. The estimated first two null angles of the ordinary pattern are $\varphi_{NL1} = -34.56°$ and $\varphi_{NL2} = 41.04°$. Consequently, the desired array pattern, $AF_d(\varphi)$ is defined according to Eq. (4) and the number of samples is set to $N = 1000$ samples. The synthesized patterns using the proposed algorithm and the GA based algorithm compared to the ordinary pattern are shown in Fig. 4. The resultant maximum SLL, HPBW, and DRR are listed in Table 1. It is clear that the proposed algorithm provides the lowest SLL and the same HPBW as the ordinary pattern. However, the DRR of the proposed algorithm is slightly greater than that of the GA. Also, it provides about 256.78% reduction in the SLL while the GA provides only 56.60% reduction in the SLL. Using the same number of samples $N = 1000$, the estimated execution time of the proposed algorithm is 0.16163 sec which is much lower than the execution time of the GA based algorithm which equals 320.2466 sec. The polar coordinates $(r_k\psi_k)$ and nodes energy transmissions (δ_k) of the synthesized patterns are tabulated in Table 2.
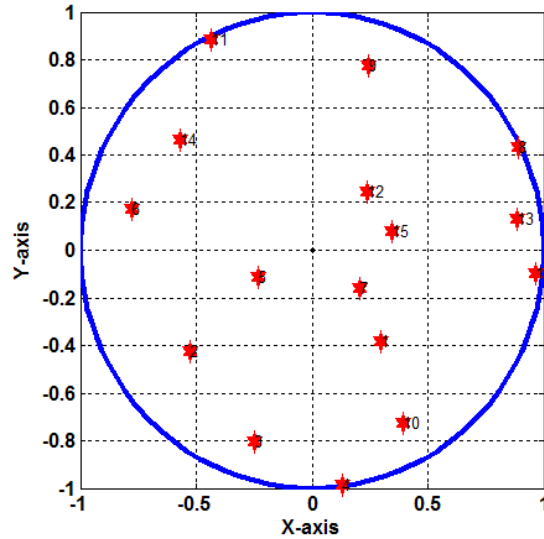
Figure 3. The nodes distribution for $K = 16$ and $R = 1\,\mathrm{m}$.

Table 1. The resultant maximum SLL, HPBW, DRR, and execution time of the proposed algorithm and the GA compared to the ordinary pattern for $K = 16$ and $R = 1\,\mathrm{m}$.

Algorith	Maximum SL	HPBW	DRR	Execution time
Ordinary Pattern	$-8.9428\,\mathrm{dB}$	$28.44°$	1	–
Proposed Algorithm	$-31.9066\,\mathrm{dB}$	$28.44°$	19.5920	$0.16163\,\mathrm{sec}$
GA [9, 10]	$-14.0047\,\mathrm{dB}$	$30.96°$	14.8762	$320.2466\,\mathrm{sec}$

Table 2. The polar coordinates (r_k, ψ_k) and nodes energy transmissions (δ_k) of the synthesized pattern for $K = 16$ and $R = 1\,\text{m}$.

k	Polar coordinates		Nodes energy transmissions (δ_k)		
k	r_k	ψ_k	Ordinary	Proposed Algorithm	GA
1	0.4842	−0.914	1	15.7500∠0.2129	0.9978
2	0.6779	0.6792	1	29.7940∠ − 0.6868	0.9542
3	0.8411	1.2698	1	4.6343∠−3.1496	0.2946
4	0.9956	−1.440	1	1.8428∠ − 6.0317	0.2378
5	0.2612	0.4538	1	26.9703∠−5.5416	0.2100
6	0.7952	−0.219	1	36.1041∠ − 8.4292	0.5661
7	0.2640	−0.660	1	24.8261∠ − 10.8984	0.2108
8	0.9916	0.4501	1	7.4936∠ − 9.4163	0.9451
9	0.8105	1.2628	1	6.5367∠ − 6.3128	0.4485
10	0.8275	−1.077	1	8.3310∠ − 4.6522	0.0671
11	0.9862	−1.113	1	4.8548∠ − 7.7595	0.4811
12	0.3394	0.7940	1	15.0842∠ − 4.9390	0.7645
13	0.8955	0.1461	1	24.2017∠−2.9559	0.1962
14	0.7340	−0.677	1	14.6938∠ − 0.9781	0.8216
15	0.3555	0.2202	1	7.1869∠−3.1065	0.1985
16	0.9713	−0.103	1	3.3245∠ − 5.8279	0.4555

Test case (2): in this case, consider a ($K = 32$ and $R = 4\,\text{m}$) RAA whose main beam is directed at the azimuth angle $\varphi_0 = 0°$ as shown in Fig. 5. The first two null angles of the ordinary pattern are $\varphi_{NL1} = -8.68°$ and $\varphi_{NL2} = 8.28°$. Fig. 6 shows the synthesized patterns using the proposed algorithm and the GA compared to the ordinary pattern, and the resultant maximum SLL, HPBW, and DRR are listed in Table 3. The percentages of SLL reduction are 88.36% and 42.98% for the proposed algorithm and the GA based algorithm respectively. The execution time of the proposed algorithm is 0.2523 sec while the execution time of the GA equals 565.0136 sec. Furthermore, the DRR of the proposed algorithm is smaller than that of the GA. The polar coordinates (r_k, ψ_k) and nodes energy transmissions (δ_k) of the synthesized patterns are listed in Table 4 and Table 5, respectively.

Table 3. The resultant maximum SLL, HPBW, DRR, and execution time of the proposed algorithm and the GA compared to the ordinary pattern for $K = 32$ and $R = 4\,\text{m}$.

Algorith	Maximum SL	HPBW	DRR	Execution time
Ordinary Pattern	−8.9381 dB	7.56°	1	−
Proposed Algorithm	−16.8359 dB	7.56°	17.9752	0.2523 sec
GA [6, 7]	−12.7795 dB	8.28°	187.0206	565.0136 sec

Test case (3): in this case, consider a RAA whose parameters are ($K = 64$ and $R = 6\,\text{m}$) as shown in Fig. 7. The direction of the intended receiver is at $\varphi_0 = 0°$. The estimated first two null angles are $\varphi_{NL1} = -6.84°$ and $\varphi_{NL2} = 6.84°$. Fig. 8 shows the synthesized patterns using the proposed algorithm and the GA compared to the ordinary pattern. The resultant maximum SLL, HPBW, and DRR are listed in Table 6. The proposed algorithm and the GA provide SLL reduction about 116.83% and 34.19% respectively. The proposed algorithm provides a suitable DRR which is smaller than that of the GA. The execution time of the proposed algorithm is 0.259299 sec which is much lower than the execution time of the GA which equals 1721.023 sec. The polar coordinates (r_k, ψ_k) and nodes energy
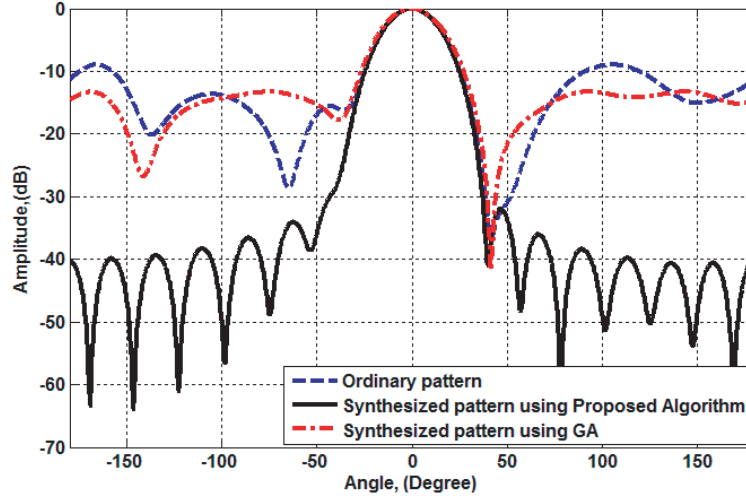
Figure 4. The synthesized patterns using the proposed algorithm and the GA compared to the ordinary pattern for $K = 16$ and $R = 1$ m.
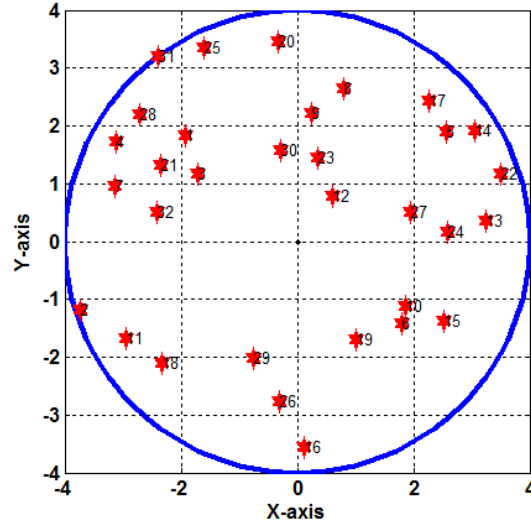

Figure 5. The nodes distribution for $K = 32$ and $R = 4$ m.

transmissions (δ_k) of the synthesized patterns are listed in Table 7, Table 8, and Table 9, respectively.

   Test case (4): in this case, the proposed algorithm is compared with the NSGA-SD algorithm introduced in [13] for synthesizing a RAA whose parameters are ($K = 8$ and $R = 4$ m) as shown in Fig. 9. Fig. 10 shows the synthesized patterns using the proposed algorithm and NSGA-SD compared to the ordinary pattern. The resultant maximum SLL, HPBW, and DRR are listed in Table 10. The simulation results revealed that the proposed algorithm outperforms the NSGA-SD algorithm in terms of maximum SLL reduction and HPBW. It provides SLL reduction of about 123.97% while the NSGA-SD provides a few reduction of about 42.76%. Also, the proposed algorithm provides the same HPBW as the ordinary pattern while the NSGA-SD algorithm provides HPBW which is slightly greater than that of the ordinary pattern. Furthermore, using the same number of samples $N = 1000$ samples, the proposed algorithm provides a very small execution time of 0.09438 sec which is much lower than the execution time of the NSGA-SD algorithm which equals 10 sec. The polar coordinates (r_k, ψ_k) and nodes transmission weights $(\mathbf{v_k})$ of the synthesized patterns are listed in Table 11.
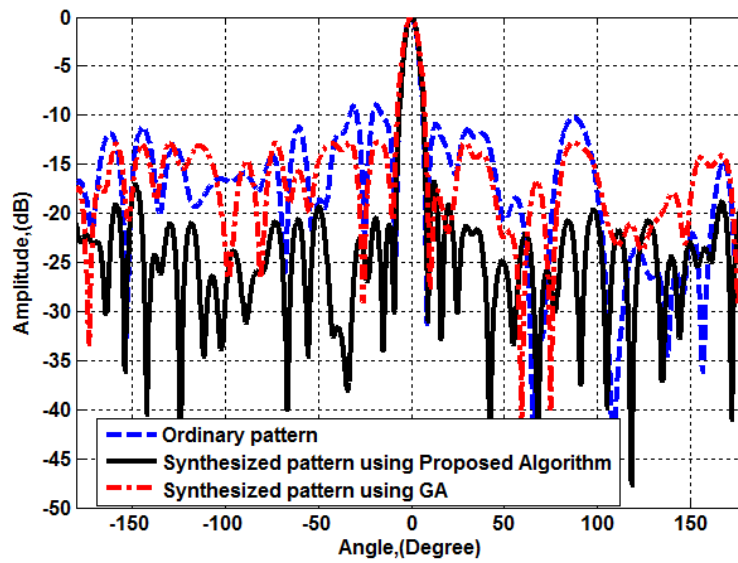
Figure 6. The synthesized patterns using the proposed algorithm and the GA compared to the ordinary pattern for $K = 32$ and $R = 4\,\text{m}$.

Table 4. The polar coordinates (r_k, ψ_k) and nodes energy transmissions (δ_k) of the synthesized pattern for $K = 32$ and $R = 4\,\text{m}$.

Polarcoordinates			Nodes energy transmissions (δ_k)		
k	r_k	ψ_k	Ordinary	Proposed Algorithm	GA
1	2.6553	-0.757	1	$0.9140\angle 0.8556$	0.3433
2	3.9234	0.3059	1	$0.6666\angle -0.3410$	0.9521
3	2.0722	-0.591	1	$0.5477\angle 0.2746$	0.0053
4	3.5536	-0.505	1	$0.6914\angle -1.1944$	0.1701
5	3.1862	0.6389	1	$0.5505\angle -1.1972$	0.0484
6	2.2991	-0.669	1	$0.1842\angle 1.3524$	0.0100
7	3.2846	-0.296	1	$1.3402\angle -0.3347$	0.7344
8	2.7649	1.2815	1	$1.8963\angle 1.7440$	0.1082
9	2.2200	1.4641	1	$3.3109\angle -0.6330$	0.5389
10	2.1880	-0.544	1	$0.4172\angle -1.3665$	0.5891
11	3.3880	0.5188	1	$1.4029\angle 0.7994$	0.4571
12	0.9962	0.9142	1	$0.9722\angle -2.5973$	0.3741
13	3.2684	0.1062	1	$1.6215\angle 0.2036$	0.9758
14	3.6165	0.5609	1	$1.0629\angle 0.9961$	0.7570
15	2.8659	-0.499	1	$0.9242\angle 1.7201$	0.6325
16	3.5685	-1.539	1	$0.9499\angle -0.9651$	0.2144

4.2. Side Lobe Level Analysis

In this section, the resultant SLL is examined under the impact of the variations in the number of nodes, K and the circular area radius R.

    Case (1): in this case, the maximum SLL versus K over the same disk radius $R = 1\,\text{m}$ is estimated for an intended receiver located at $\varphi_0 = 0°$. The resultant maximum SLL using the proposed algorithm,

Table 5. The polar coordinates (r_k, ψ_k) and nodes energy transmissions (δ_k) of the synthesized pattern for $K = 32$ and $R = 4$ m.

| Polarcoordinates			Nodes energy transmissions (δ_k)		
k	**r_k**	**ψ_k**	**Ordinary**	**Proposed Algorithm**	**GA**
17	3.3281	0.8202	1	1.2163∠2.1403	0.1399
18	3.1480	0.7378	1	0.8306∠2.5130	0.0588
19	1.9732	−1.038	1	0.8169∠4.4694	0.0703
20	3.4765	−1.474	1	0.8774∠6.7142	0.1972
21	2.6898	−0.509	1	0.9463∠6.4790	0.8445
22	3.7000	0.3214	1	0.4570∠6.7499	0.9331
23	1.4750	1.3368	1	2.0058∠5.0911	0.5518
24	2.5896	0.0592	1	0.9423∠6.0520	0.9999
25	3.7174	−1.125	1	0.9521∠6.9203	0.2661
26	2.7914	1.4638	1	2.0410∠5.2970	0.5470
27	2.0031	0.2580	1	0.9731∠6.4173	0.6557
28	3.4931	−0.676	1	1.4351∠6.0215	0.9976
29	2.1547	1.2081	1	1.1327∠7.9586	0.3310
30	1.5932	−1.387	1	0.2206∠6.6079	0.8130
31	3.9965	−0.927	1	0.4402∠6.2421	0.7302
32	2.4736	−0.207	1	0.9784∠6.5731	0.7308
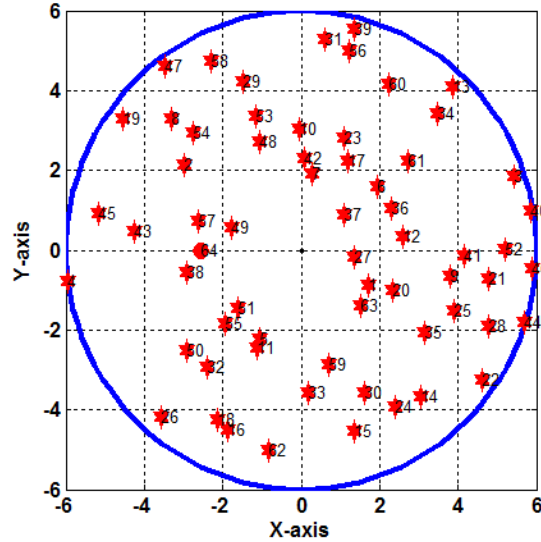
Figure 7. The nodes distribution for $K = 64$ and $R = 6$ m.

GA, and the ordinary pattern are shown in Fig. 11. The simulation results revealed that the proposed algorithm outperforms the GA technique as it provides maximum SLL range (from -31.9066 dB to -40.3119 dB) when K changes from ($K = 16$ to $K = 80$). However, the ordinary pattern and the GA provide maximum SLL range (from -8.9428 dB to -14.7544 dB) and (from -14.0047 dB to -32.3507 dB), respectively.

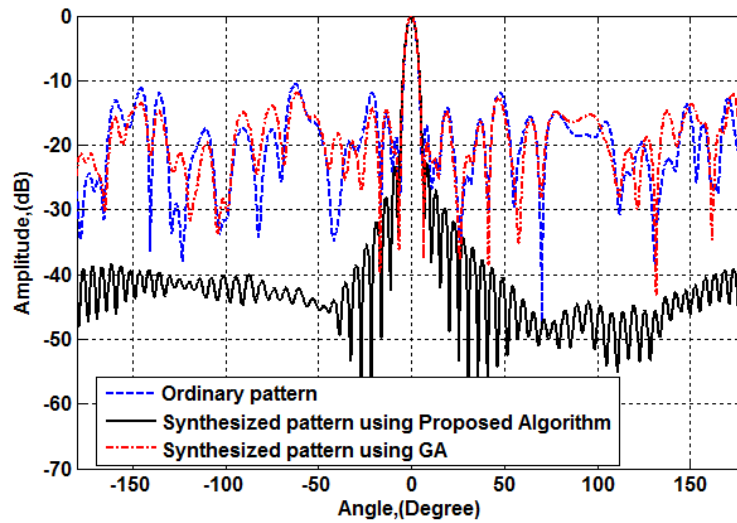   ***Case (2):*** in this case, for a fixed number of the distributed nodes $K = 16$, the maximum SLL

Figure 8. The synthesized patterns using the proposed algorithm and the GA compared to the ordinary pattern for $K = 64$ and $R = 6\,\text{m}$.

Table 6. The resultant maximum SLL, HPBW, DRR, and execution time of the proposed algorithm and the GA compared to the ordinary pattern for $K = 64$ and $R = 6\,\text{m}$.

Algorith	Maximum SL	HPBW	DRR	Execution time
Ordinary Pattern	$-10.5482\,\text{dB}$	$5.4°$	1	–
Proposed Algorithm	$-22.8713\,\text{dB}$	$5.4°$	23.1860	$0.259299\,\text{sec}$
GA [9, 10]	$-12.8419\,\text{dB}$	$5.5°$	62.8482	$1721.023\,\text{sec}$

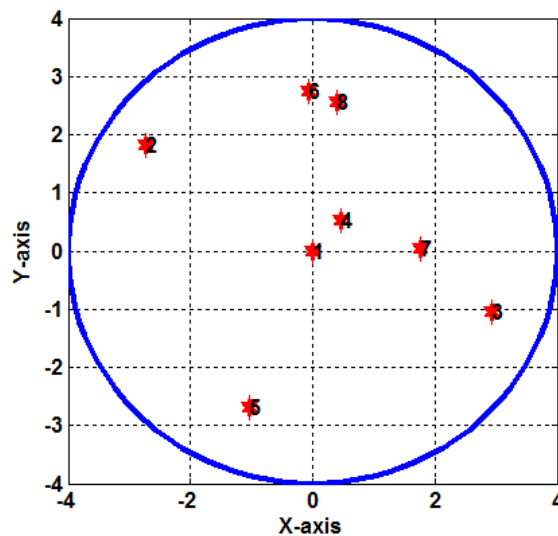**Figure 9.** The nodes distribution for $K = 8$ and $R = 4\,\text{m}$.

versus disk radius R is estimated for an intended receiver located at $\varphi_0 = 0°$. Fig. 12 shows the resultant maximum SLL using the proposed algorithm, GA, and the ordinary pattern over the disk radius range ($R = 1\,\text{m}$ to $10\,\text{m}$). Also, it is clear that the proposed algorithm provides the highest performance over

the entire range of disk radius. It provides maximum SLL range (from $-31.9066\,\text{dB}$ to $-7.8920\,\text{dB}$) when the disk radius R changes from ($R = 1\,\text{m}$ to $10\,\text{m}$). However, the ordinary pattern and the GA provide maximum SLL ranges (from $-8.9428\,\text{dB}$ to $-3.9208\,\text{dB}$) and (from $-14.0047\,\text{dB}$ to $-5.5796\,\text{dB}$) respectively.

Table 7. The polar coordinates (r_k, ψ_k) for $K = 64$ and $R = 6\,\text{m}$.

Polarcoordinates											
k	**r_k**	**ψ_k**	**k**	**r_k**	**ψ_k**	**k**	**r_k**	**ψ_k**	**k**	**r_k**	**ψ_k**
1	1.9157	−0.471	17	2.5249	1.0758	33	3.5861	−1.521	49	1.8737	−0.303
2	3.6516	−0.621	18	4.7466	1.1031	34	4.8725	0.7798	50	3.8408	0.7141
3	5.7384	0.3249	19	5.6172	−0.6290	35	3.7670	−0.584	51	2.1731	0.7369
4	5.9970	0.1321	20	2.5328	−0.405	36	2.5348	0.4253	52	5.2119	0.0044
5	2.4775	1.1248	21	4.8209	−0.149	37	1.3981	0.6896	53	3.5400	−1.236
6	2.4928	0.6844	22	5.6417	−0.614	38	2.9827	0.1857	54	4.0240	−0.822
7	1.9263	1.4323	23	3.0031	1.1940	39	5.6978	1.3289	55	2.6788	0.7561
8	4.6713	−0.779	24	4.5939	−1.023	40	5.9471	0.1632	56	5.1492	1.3315
9	3.8507	−0.167	25	4.1866	−0.370	41	4.1747	−0.036	57	2.7058	0.2669
10	3.0345	−1.556	26	5.4961	0.8670	42	2.2828	1.5371	58	5.2587	−1.116
11	2.6946	1.1376	27	1.3639	−0.123	43	4.2919	−0.111	59	2.9472	−1.325
12	2.5994	0.1341	28	5.1596	−0.379	44	5.9806	−0.305	60	4.7005	−1.077
13	5.6406	0.8122	29	4.4680	−1.232	45	5.2395	−0.178	61	3.5281	0.6887
14	4.7677	−0.879	30	3.9320	−1.145	46	5.8972	−0.078	62	5.1005	1.4072
15	4.7336	−1.277	31	5.2981	1.4547	47	5.7858	−0.924	63	2.0543	−0.737
16	4.8680	1.1787	32	3.7789	0.8876	48	2.9178	−1.199	64	2.5512	0.0031

Table 8. The nodes energy transmissions (δ_k) of the synthesized pattern for $K = 64$ and $R = 6\,\text{m}$.

Nodes energy transmissions (δ_k)							
k	**Ordinary**	**Proposed Algorithm**	**GA**	**k**	**Ordinary**	**Proposed Algorithm**	**GA**
1	1	7.3130∠ − 2.2610	0.8607	17	1	32.9661∠ − 1.7764	0.8589
2	1	34.9493∠ − 2.3199	0.5446	18	1	1.7948∠ − 4.1720	0.1068
3	1	28.0571∠ − 0.9256	0.2117	19	1	14.6898∠ − 5.3713	0.7646
4	1	2.3330∠1.7749	0.0801	20	1	30.3403∠ − 7.4535	0.4388
5	1	36.7422∠2.1666	0.5406	21	1	34.3154∠ − 8.0161	0.4295
6	1	14.0118∠4.9403	0.8883	22	1	2.1285∠−7.1076	0.0578
7	1	10.6703∠2.7589	0.7297	23	1	20.6731∠ − 4.8484	0.1366
8	1	18.1557∠ − 0.4330	0.5311	24	1	11.7723∠ − 3.8676	0.2403
9	1	31.4089∠0.0851	0.7362	25	1	27.0197∠ − 4.5441	0.0158
10	1	5.1443∠ − 0.5024	0.4748	26	1	3.1625∠ − 4.7318	0.9937
11	1	19.5027∠0.8992	0.3001	27	1	4.5873∠−3.9360	0.4950
12	1	5.1431∠0.8692	0.4856	28	1	36.4125∠ − 5.0029	0.4771
13	1	6.6639∠ − 0.6234	0.5951	29	1	11.5907∠ − 6.5602	0.6842
14	1	10.6357∠ − 2.6139	0.5870	30	1	14.0783∠ − 3.5431	0.9723
15	1	5.0176∠ − 2.6889	0.8266	31	1	1.5847∠−6.4193	0.8291
16	1	2.4591∠ − 4.0906	0.5432	32	1	9.1922∠ − 3.3820	0.9717

Table 9. The nodes energy transmissions (δ_k) of the synthesized pattern for $K = 64$ and $R = 6$ m.

Nodes energy transmissions (δ_k)						
k	Ordinary	Proposed Algorithm	GA	k	Ordinary	Proposed Algorithm	GA
33	1	$2.3079\angle - 6.8117$	0.1726	49	1	$3.9142\angle - 11.3588$	0.7557
34	1	$16.5709\angle - 7.0848$	0.9876	50	1	$20.7471\angle - 12.0369$	0.9212
35	1	$36.6102\angle - 6.6202$	0.7685	51	1	$28.2178\angle - 10.1590$	0.8000
36	1	$28.5454\angle - 9.2038$	0.7136	52	1	$8.9211\angle - 12.0014$	0.8768
37	1	$25.1721\angle - 5.8573$	0.9249	53	1	$11.8328\angle - 11.4923$	0.3159
38	1	$12.5651\angle - 6.6190$	0.9840	54	1	$5.1548\angle - 11.3130$	0.2939
39	1	$1.5942\angle - 7.0245$	0.2941	55	1	$20.9906\angle - 12.3521$	0.6820
40	1	$20.2395\angle - 6.8799$	0.9397	56	1	$2.2180\angle - 12.3755$	0.0664
41	1	$24.6302\angle - 9.6349$	0.3558	57	1	$5.0911\angle - 15.6113$	0.2043
42	1	$4.0354\angle - 7.8365$	0.4616	58	1	$4.2611\angle - 12.8152$	0.2024
43	1	$16.3730\angle - 9.4768$	0.0829	59	1	$26.4804\angle - 14.6527$	0.6462
44	1	$12.6796\angle - 9.5369$	0.4293	60	1	$3.0665\angle - 14.3484$	0.1310
45	1	$29.0337\angle - 10.6186$	0.4842	61	1	$29.6211\angle - 14.6274$	0.0178
46	1	$3.7763\angle - 9.7732$	0.5034	62	1	$2.4838\angle - 16.8718$	0.6771
47	1	$3.0559\angle - 11.5927$	0.5997	63	1	$26.0455\angle - 18.5841$	0.8941
48	1	$5.4749\angle - 14.6929$	0.7557	64	1	$11.4999\angle - 18.4030$	0.7483

Table 10. The resultant maximum SLL, HPBW, and DRR of the proposed algorithm and the NSGA-SD compared to the ordinary pattern for $K = 8$ and $R = 4$ m.

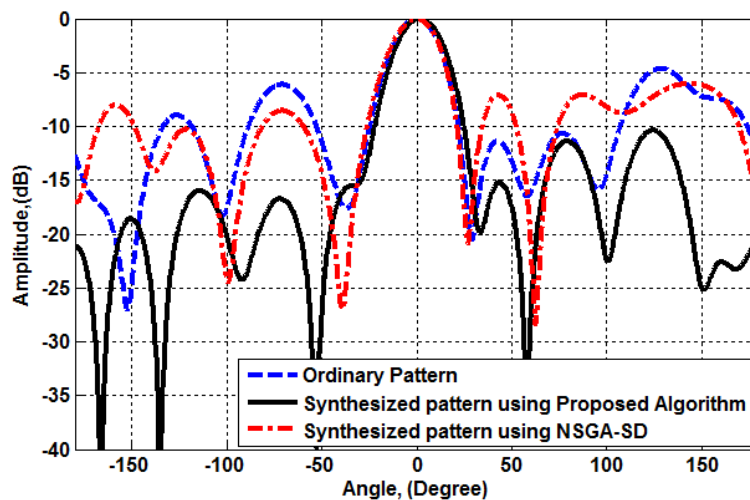| Algorith	Maximum SL	HPBW	DRR	Execution time
Ordinary Pattern	-4.63 dB	$12.20°$	1	–
Proposed Algorithm	-10.37 dB	$12.20°$	3.0685	0.09438 sec
NSGA-SD [13]	-6.61 dB	$12.35°$	2.0625	10 sec

Figure 10. The synthesized patterns using the proposed algorithm and the NSGA-SD compared to the ordinary pattern for $K = 8$ and $R = 4$ m.

Table 11. The polar coordinates (r_k, ψ_k) and nodes transmission weights $(\mathbf{v_k})$ of the synthesized pattern for $K = 8$ and $R = 4\,\mathrm{m}$.

| Polar coordinates			Nodes transmissions weight $(\mathbf{v_k})$		
k	$\mathbf{r_k}$	$\psi_\mathbf{k}$	Ordinary	Proposed Algorithm	$\mathbf{NSGA - SD}$
1	0	0	$1\angle 0.12$	$1.2661\angle -0.6484$	$0.53\angle 0.18$
2	3.2755	0.5855	$1\angle 1.31$	$0.5252\angle 0.5315$	$0.94\angle 1.10$
3	3.1219	-0.343	$1\angle -0.69$	$0.4938\angle -1.158$	$0.31\angle -1.12$
4	0.6868	0.8369	$1\angle 0.10$	$1.5151\angle 0.8978$	$0.19\angle 0.05$
5	2.8898	1.2064	$1\angle -1.73$	$1.1818\angle -1.2798$	$0.76\angle -1.03$
6	2.7509	-1.545	$1\angle 2.19$	$0.6784\angle 2.2068$	$0.56\angle 2.05$
7	1.7605	0.0227	$1\angle -0.12$	$0.8861\angle 0.3869$	$0.97\angle 0.01$
8	2.5911	1.4158	$1\angle 0.04$	$1.1477\angle -0.5825$	$0.72\angle 0.16$
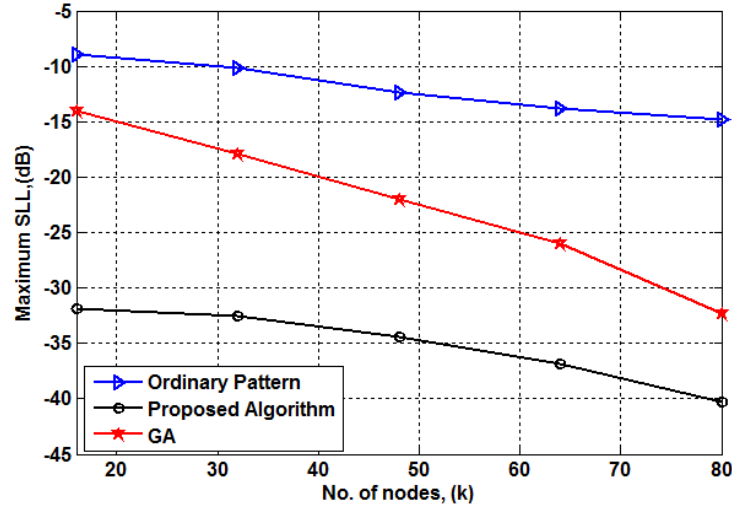
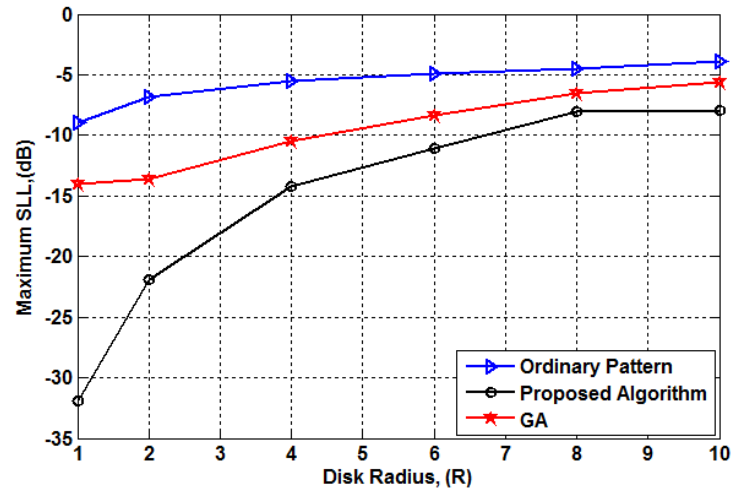**Figure 11.** The maximum SLL versus K for $R = 1\,\mathrm{m}$.

Figure 12. The maximum SLL versus R for $K = 16$.

5. CONCLUSION

In this paper, a fast deterministic distributed beamforming algorithm is proposed for maximum SLL reduction of RAAs in wireless sensor networks. It controls the energy transmission δ_k or transmission weight ($\mathbf{v_k}$) of each node without altering the nodes locations. The simulation results verify the feasibility and effectiveness of the proposed algorithm compared to the recent state of the art GA and NSGA-SD optimization based techniques. It provides the highest SLL reduction while maintaining the same HPBW as the ordinary pattern. Furthermore, it is not time consuming which makes it suitable for adaptive beamforming of distributed random antenna arrays.

REFERENCES

1. Bhattacharyya, K., *Phased Array Antennas: Floquet Analysis, Synthesis, BFNs and Active Array Systems*, John Wiley & Sons, 2006.

2. Adachi, F., W. Peng, T. Obara, T. Yamamoto, R. Matsukawa, and S. Nakada, "Distributed antenna network for gigabit wireless access," *International Journal of Electronics and Communications (AEÜ)*, Vol. 66, No. 8, 605–612, 2012.

3. Jung, S. Y. and B. W. Kim, "Near-optimal low-complexity antenna selection scheme for energy-efficient correlated distributed MIMO systems," *International Journal of Electronics and Communications (AEÜ)*, Vol. 69, No. 7, 1039–1046, 2015.

4. Valenzuela-Valdes, J., F. Luna, R. Luque-Baena, and P. Padilla, "Saving energy in WSNs with beamforming," *IEEE, International Conference on Cloud Networking*, 255–260, 2014.

5. Ochiai, H., P. Mitran, H. V. Poor, and V. Tarokh, "Collaborative beamforming for distributed wireless ad hoc sensor networks," *IEEE Transactions on Signal Processing*, Vol. 53, No. 11, 4110–4124, 2005.

6. Jayaprakasam, S., S. K. A. Rahim, and C. Y. Leow, "Distributed and collaborative beamforming in wireless sensor networks: Classifications, trends, and research directions," *IEEE Communications Surveys & Tutorials*, Vol. 19, No. 4, 2092–2116, 2017.

7. Ahmed, M. F. and S. A. Vorobyov, "Sidelobe control in collaborative beamforming via node selection," *IEEE Transactions on Signal Processing*, Vol. 58, No. 12, 6168–6180, 2010.

8. Liang, S., T. Feng, G. Sun, J. Zhang, and H. Zhang, "Transmission power optimization for reducing sidelobe via bat-chicken swarm optimization in distributed collaborative beamforming," *IEEE International Conference on Computer and Communications (ICCC)*, 2164–2168, 2016.

9. Jayaprakasam, S., S. Rahim, L. C. Yen, and K. Ramanathan, "Genetic algorithm based weight optimization for minimizing sidelobes in distributed random array beamforming," *IEEE International Conference on Parallel and Distributed Systems*, 623–627, 2013.

10. Jayaprakasam, S., S. K. A. Rahim, C. Y. Leow, and T. O. Ting, "Sidelobe reduction and capacity improvement of open-loop collaborative beamforming in wireless sensor networks," *PloS one*, Vol. 12, No. 5, 1–33, 2017.

11. Jayaprakasam, S., S. K. A. Rahim, C. Y. Leow, and M. F. M. Yusof, 'Beampatten optimization in distributed beamforming using multiobjective and metaheuristic method," *IEEE Symposium on Wireless Technology and Applications (ISWTA)*, 86–91, 2014.

12. Jayaprakasam, S., S. Rahim, and C. Y. Leow, "PSOGSA-explore: A new hybrid metaheuristic approach for beampattern optimization in collaborative beamforming," *Applied Soft Computing*, Vol. 30, 229–237, 2015.

13. Jayaprakasam, S., S. K. A. Rahim, C. Y. Leow, T. O. Ting, and A. A. Eteng, "Multiobjective beampattern optimization in collaborative beamforming via NSGA-II with selective distance," *IEEE Transactions on Antennas and Propagation*, Vol. 65, No. 5, 2348–2357, 2017.

14. Shi, W., Y. Li, L. Zhao, and X. Liu, "Controllable sparse antenna array for adaptive beamforming," *IEEE Access*, Vol. 7, 6412–6423, 2019.

15. Li, Y., Y. Wang, and T. Jiang, "Norm-adaption penalized least mean square/fourth algorithm for sparse channel estimation," *Signal Processing*, Vol. 128, 243–251, 2016.

16. Li, Y., Y. Wang, and T. Jiang, "Sparse-aware set-membership NLMS algorithms and their application for sparse channel estimation and echo cancelation," *AEU — International Journal of Electronics and Communications*, Vol. 70, No. 7, 895–902, 2016.

17. Li, Y., Z. Jiang, W. Shi, X. Han, and B. Chen, "Blocked maximum correntropy criterion algorithm for cluster-sparse system identifications," *IEEE Transactions on Circuits and Systems II: Express Briefs*, 2109.

18. Yu, K., Y. Li, and X. Liu, "Mutual coupling reduction of a MIMO antenna array using 3-D novel meta-material structures," *Applied Computational Electromagnetics Society Journal*, Vol. 33, No. 7, 758–763, 2018.

19. Jiang, T., T. Jiao, and Y. Li, "A low mutual coupling MIMO antenna using periodic multi-layered electromagnetic band gap structures," *Applied Computational Electromagnetics Society Journal*, Vol. 33, No. 3, 305–311, 2018.